A reporter system evaluates tumorigenesis, metastasis, β-catenin/MMP regulation, and druggability

Chiharu Sogawa[1,¶], Takanori Eguchi[1,2,¶,*], Yuka Okusha[1], Kisho Ono[1], Kazumi Ohyama[1], Motoharu Iizuka[3], Ryu Kawasaki[3], Yusaku Hamada[3], Masaharu Takigawa[2], Norio Sogawa[4], Kuniaki Okamoto[1], and Ken-ichi Kozaki[1]

[1]Department of Dental Pharmacology, Graduate School of Medicine, Dentistry and Pharmaceutical Sciences, Okayama University, Okayama, Japan, 700-8525.
[2]Advanced Research Center for Oral and Craniofacial Sciences, Graduate School of Medicine, Dentistry and Pharmaceutical Sciences, Okayama University, Okayama, Japan, 700-8525.
[3]Research program for undergraduate students, Okayama University Dental School, Okayama, Japan, 700-8525.
[4]Department of Dental Pharmacology, Matsumoto Dental University, Shiojiri, Japan, 399-0704.
[¶]These authors contributed to this work equally.

*Correspondence: Takanori Eguchi. 2-5-1, Shikata-cho, Okayama, 700-8525, Japan. E-mail: eguchi@okayama-u.ac.jp

Running title: Novel reporter system evaluates malignancy and druggability

Abstract

Cancer invasion, metastasis, and therapy resistance are the crucial phenomena in cancer malignancy. The high-expression of matrix metalloproteinase 9 (MMP9) is a biomarker as well as a causal factor of cancer invasiveness and metastatic activity. However, a regulatory mechanism underlying MMP9 expression in cancer is not clarified yet. Additionally, a new strategy for anti-cancer drug discovery is becoming an important clue. In the present study, we aimed (i) to develop a novel reporter system evaluating tumorigenesis, invasiveness, metastasis, and druggability with a combination of three-dimensional (3D) tumoroid model and *Mmp9* promoter and (ii) to examine pharmacological actions of anti-cancer medications using this reporter system. High expression and genetic amplification of *MMP9* were found in colon cancer cases. We found that proximal promoter sequences of *MMP9* in murine and human contained conserved binding sites for transcription factors β-catenin/TCF/LEF, glucocorticoid receptor (GR), and NF-κB. The murine *Mmp9* promoter (-569 to +19) was markedly activated in metastatic colon cancer cells and additionally activated by tumoroid formation and by β-catenin signaling stimulator lithium chloride (LiCl). The *Mmp9* promoter-driven fluorescent reporter cells enabled the monitoring of activities of MMP9/gelatinase, tumorigenesis, invasion, and metastasis in syngeneic transplantation

1

experiments. We also demonstrated pharmacological actions as follows. ids Dexamethasone and hydrocortisone, steroidal medications binding to GR, inhibited the *Mmp9* promoter but did not inhibit tumorigenesis. On the other hand, an antimetabolite 5-fluorouracil, a golden standard for colon cancer chemotherapy, inhibited tumoroid formation but did not inhibit *Mmp9* promoter activity. Notably, anti-malaria medication artesunate inhibited both tumorigenesis and the *Mmp9* promoter in vitro, potentially through inhibition of β-catenin/TCF/LEF signaling. Thus, this novel reporter system enabled monitoring tumorigenesis, invasiveness, metastasis, key regulatory signalings such as β-catenin/MMP9 axis, and druggability.

Impact Statement

Cancer invasion and metastasis have been shown to be driven by MMP9, whose expression mechanism is not clarified yet. Additionally, a new strategy for anti-cancer drug discovery is becoming important. We established a novel reporter system evaluating tumorigenesis, invasiveness, metastasis, and druggability with a combination of 3D tumoroid model and *Mmp9* promoter. Using this reporter system, we demonstrated pharmacological actions of anti-cancer medications such as an antimetabolite 5-fluorouracil and anti-malaria medication artesunate, which inhibited both tumorigenesis and β-catenin/MMP regulatory signaling. Our study impacts the translational fields of oncology, drug discovery, and organoid model.

Introduction

Cancer is one of the most serious diseases all over the world, and its metastasis and therapy resistance are leading causes of death. A new strategy for anti-cancer drug discovery is becoming an important clue. Success in the anti-cancer drug discovery depends on the appropriate experimental tumor models and screening system. Organoid model and tissue engineering have been devised by scientific/medical motivation for regenerative medicine and drug discovery. In the field of cancer study, three-dimensional (3D) spheroid/tumoroid culture system has enabled us to develop tumor-like organoid (tumoroid) *in vitro*, which correspond closely to native tumors *in vivo* (1-9). Matrix metalloproteinases (MMPs) represent the most prominent family of proteinases associated with tumorigenesis (10), tumor microenvironment (11), angiogenesis (12, 13), migration, invasion (14), and metastasis (10). Canonical roles for MMPs are to cleave and proteolyze substrate proteins at extracellular space. Proteolysis of extracellular matrix (ECM) and intercellular adhesion molecules by MMPs increase cellular motility, migration and invasion abilities (15). Proteolysis of ECM also promotes the release of cytokines, chemokines, and growth factors that activate their receptors and intracellular signaling pathways. MMPs also directly alter the activities of growth factors, cytokines, and chemokines by proteolysis (16). High expression of MMP9 and MMP3 has been reported in human colon cancer in late stages with poor prognosis of patients (17-19). We recently showed that MMP9 and MMP3 are markedly produced by rapidly metastatic colon cells and targeted depletion of these MMPs successfully inhibited tumor growth, invasion, and metastasis (10). Additionally, intracellular MMPs play key roles in transcriptional regulation (20-22), intracellular proteolysis, and migration of cancer cells (10). These studies prompted us to pursue

potential signals contributing to the high-expression of MMP9, whose promoter is markedly activated in metastatic cancer cells in vivo and in vitro. We also aimed to utilize the powerful MMP9 promoter for monitoring tumorigenic, invasive and metastatic activities of cancer cells as well as the development of a novel drug discovery system.

Drug screening, as well as tissue/cell culture, had been often carried out using two-dimensional (2D) monolayer culture on plastic plates, which unintentionally altered characteristics of the cells. For example, 2D culture markedly induces forced expression of integrins, which is required for attachment to such plate materials (23). In contrast, 3D organoid/tissue culture systems are able to replicate many aspects of 3D organs, tumors, and their environment and are thus more suitable for many physiological and pathological studies (1, 24, 25). One of such features of 3D organogenesis is an enhancement of stem-cell phenotype (2). We showed that 3D organoid/tumoroid culture of cancer cells enhanced stem-cell phenotype with enhanced expression of stem-cell marker genes (2). It has been also shown that tumor microenvironment consists of cancer cells including cancer-initiating cells (CIC) also known as cancer stem cells (CSC), which can play key roles in tumorigenesis, recurrence, resistance, heterogeneity, and metastatic ability (26). The features of stem cells in both organogenesis and tumorigenesis have been shown mediated by Wnt/β-catenin/TCF signal (27-30). Wnt/β-catenin/TCF signaling is often activated in colon cancer by mutations in β-catenin or adenomatous polyposis coli (APC), a repressive cofactor of β-catenin (31). β-catenin appears to control renewal of the CIC/CSC fraction through regulation of proteins such as cyclin D1 (32, 33). β-catenin is also regulated by control of its rate of degradation that is mediated through phosphorylation by the kinase GSK3 on an N-terminal destruction motif. Binding of the ligand Wnt to surface receptors Frizzled and LRP-5/6 triggers Dsh to inhibit GSK3 activity, prevents the degradation and permits the influence of β-catenin in CIC/CSC renewal (34). By analyzing *Mmp9* promoter sequence, we found a β-catenin/TCF binding motif is conserved between human and mouse in the proximal promoter sequences of *MMP9*. In the present study, we therefore aimed to investigate β-catenin/TCF/MMP9 regulatory axis in tumorigenesis.

The 3D culture system-based organoid/tumoroid formation is a general interest as well as useful for drug screening that targets resistant tumorigenesis with enhanced CIC/CSC phenotypes (2, 25). We in the present study examined whether 5-fluorouracil (5-FU), hydrocortisone (HC), and artesunate (ART) could inhibit in vitro tumorigenesis. 5-FU is the first-choice drug in the treatment of colon cancer due to its ability to inhibit the growth of cancer cells by incorporating its metabolites into DNA and RNA (35). ART is part of the artemisinin group of drugs that treat malaria and is also active against cancer (36). Recently, ART was identified as a selective inhibitor of cancer stemness (37). We therefore hypothesized that ART could inhibit resistant/recurrent tumorigenesis through inhibiting stemness. HC is the pharmaceutical term for steroid hormone cortisol, in the glucocorticoid class of hormones, used as a steroidal anti-inflammatory drug (SAID) or an immunosuppressive drug. We examine this drug, because (i) HC tended to could inhibit *in vitro* tumorigenesis in our previous study (25) and (ii) HC binding to the glucocorticoid receptor (GR) represses activities of NF-κB and AP1 (38, 39). We found consensus binding sequences of both GR and NF-κB in the *Mmp9* promoter sequence, which we hypothesized could be repressed by HC.

3

Thus, the specific aims in the present study are (i) to develop a novel reporter system with a combination of 3D tumoroid model for drug discovery, (ii) to investigate whether a novel β-catenin/MMP9 regulatory axis could contribute to tumorigenesis with enhanced stemness and (iii) to examine whether 5-FU, HC, and ART could inhibit in vitro 3D tumorigenesis in the tumoroid culture system.

Materials and Methods

Cell culture. A rapidly metastatic colon cancer cell line LuM1, its parental slowly metastatic cell line Colon26, and its none-metastatic subline NM11 (10, 40) were cultured in RPMI1640 with 10% FBS supplemented with penicillin, streptomycin, and amphotericin B or in mTeSR1 stem-cell medium (STEMCELL Technologies, Vancouver, Canada) (2, 41) on 2D tissue culture plates (Corning, Corning, NY) or NanoCulture Plates (NCPs) (MBL, Nagoya, Japan) that enable 3D culture (2, 25, 42).

Chemicals and drugs. LiCl, Dexamethasone (DEX), 12-*O*-Tetradecanoylphorbol 13-acetate (TPA) and HC were purchased from Sigma-Aldrich (St Louis, MO). ART was purchased from Cayman Chemical (Ann Arbor, MI). AG490 was purchased from Tokyo Chemical Industry (Tokyo, Japan).

RT-qPCR. RT-qPCR was performed as described (2). Total RNA was prepared from biological quadruplicates. PCR was performed in triplicate. Primers used were mMmp9-Fw, 5'-CAGCCGACTTTTGTGGTCTT-3'; mMmp9-Rv, 5'-GCTTCTCTCCCATCATCTGG-3'; mMmp2-Fw, 5'-GTCGCCCCTAAA ACAGACAA-3'; mMmp2-Rv, 5'-GGTCTCGATGGTGTTCTGGT-3'; mMmp14-Fw, 5'-CCCTTTTACCAGTGG ATGGA-3'; mMmp14-Rv, 5'-TTTGGGCTTATCTGGGACAG-3'; b-actin-Fw, 5'-AACGAGCGGTTCCGATG-3'; b-actin-Rv, 5'-GGATTCCATACCCAAGAAGGA-3'.

Promoter analysis and cloning. As described (43), murine and human *MMP9* promoter sequences were obtained from the Eukaryotic Promoter Database (EPD). Transcription factor binding sites were predicted using PROMO (ver 8.3). The two sequences were aligned using NCBI BLAST.
A 588-bp cDNA fragment of *Mmp9* promoter between -569 and +19 was cloned via genomic PCR from a tail of a BALB/c mouse using DNA isolation kit (Qiagen, Hilden, Germany) (44). A sense primer 5'-AAGGAGTCAGCCTGCTGGAGCTAGGGGTTTGC-3' and an antisense primer 5'-GGGCCCGGTGAGGACCGCAGCTTCTTCTGGCTAACGCT-3') were used for PCR, whose products were sub-cloned into TA vectors. The 588-bp *Mmp9* promoter region was cut out using *Apa*I and inserted into a pZsGreen1-1 vector (Clontech, Palo Alto, CA). This *Mmp9* promoter-driven ZsGreen reporter expression plasmid was designated pZsGreen/Mmp9-promo.

Electroporation and reporter assay. Electroporation-transfection was performed as described (1, 45). For transient transfection, 3.5×10^5 cells were transfected with 10 μg of pMmp9-ZsGreen or pCMV-GFP (NEPA Gene) using NEPA21 electroporator (NEPA Gene, Ichikawa, Japan). The condition of electroporation was optimized for Colon26 and LuM1 (1). Poring pulse condition was total two pulses at 150 V for 5 msec pulse length with 50 msec

interval between the pulses, 10% decay rate with + polarity. The transfer pulse condition was total five pulses at 20 V for 50 msec pulse length with 50 msec interval, 40% decay rate with ± polarity. After the electroporation, cells were immediately suspended into RPMI1640 10% FBS, seeded at a concentration of 1.75×10^4 cells/100 µl in a well of 96-well 2D-culture plates, and then cultured for 24 hours. Alternatively, cells were mixed with pCMV-EGFP without electroporation as a negative control. NucBlue® Hoechst33342 (Thermo Fisher Scientific, Waltham, MA) was dropped to the medium, and cells were incubated for 1 hour to count total cell number. ArrayScan™ High Content Screening (HCS) system (Thermo Fisher Scientific) was used for measurement of fluorescence (2). The rate of ZsGreen-positive cells (*Mmp9* promoter-activated cells) and *Mmp9* promoter activities were normalized with transfection efficiencies of pCMV-EGFP. *Mmp9* promoter activity was evaluated by an average fluorescence intensity per µm^2 (= pixel) of ZsGreen positive cells in a well using ArrayScan™ HCS system.

Cloning of stable transfectant cells and reporter assay. LuM1 cells grown until 60% confluency were transfected with pZsGreen/Mmp9-promo using FuGENE6 reagent (Roche, Basel, Switzerland) in a 35-mm culture dish. Cells were re-seeded at day 2 post-transfection period. G418 (0.5 mg/ml) was added a day later. Culture medium was replaced by fresh ones containing G418 every 3 days. Cells survived for 10 days were re-seeded in 96-well plates at a concentration of 0.5 cell/well. ZsGreen-positive single colonies were picked.
For reporter assay to study effects of TPA, DEX and SB431542 using the stable cells, 5.0×10^3 cells were seeded onto a 96-well 2D culture plate in RPMI1640 supplemented with 10% FBS for 24 hours, then drugs were added, and cultured for 24 hours. *Mmp9* promoter activity was evaluated by an average fluorescence intensity per µm^2 of all cells in a well. Experiments were performed with 3 or 4 biological replicates.

Gelatin zymography. As described (10), protein samples (10 µg) were mixed with an SDS sample buffer and then applied to a 10% acrylamide gel containing copolymerized 0.1% gelatin.

Invasion assay. As described (10), in vitro invasion assays were performed using Matrigel-coated culture systems (Becton Dickinson), respectively. Cells (2.5×10^4 cells) were transferred into upper chambers of transwell® 24-well (Corning). The invading cells on lower surfaces of filters were fixed at 24 hours post-cell-transfer period. Fluorescence images were taken using Floid® Cell Imaging Station (Thermo Fisher Scientific).

Syngeneic transplantation. All animal experiments were performed according to the guidelines for the care and use of laboratory animals approved by Okayama University and the Japanese Pharmacological Society (OKU-2015659). As described (10), 5×10^5 cells were transplanted subcutaneously at side abdominal walls of 6 to 7 weeks-old female BALB/c mice. The mice were fixed by perfusion fixation with 4 % paraformaldehyde at day 20 and 40 after the transplantation. The primary tumor and lungs were resected and observed under a fluorescent stereomicroscope SZX-12 (Olympus, Tokyo, Japan) at Central Research Laboratory, Okayama University Medical School.

3D tumoroid reporter assay. To investigate the effects of lithium chloride (LiCl) on the stable clone, cells were seeded at a concentration of 5×10^3 cells /well in a 96-well NCP or a 96-well 2D culture plate, and were pre-cultured in RPMI1640 with 10% FBS for 2 days, then LiCl was added and cultured in RPMI1640 with 2% or 10% FBS for 2 days. Alternatively, cells were cultured in the presence of LiCl in RPMI1640 with 2% or 10% FBS for 3 days. To investigate the effects of 5-FU, HC, ART, and AG490, cells were seeded at a concentration of 5×10^3 cells/well in a 96-well NCP and cultured in mTeSR1 for 3 days with or without drugs. For counting cell-aggregates/tumoroids, fluorescent intensity and area (μm^2= pixel) of each aggregate per well was calculated using the ArrayScan™ HCS system. Fluorescent areas greater than 300 μm^2 were counted as cell-aggregates/tumoroids. *Mmp9* promoter activity was evaluated by an average fluorescence intensity per μm^2 of all cells in a well as described above. Experiments were performed with 3 or 4 biological replicates.

Western blot analysis. Cytoplasmic and Nuclear lysate were prepared using NE-PER Nuclear and Cytoplasmic Extraction Reagents (Thermo Fisher Scientific). As described (10), protein samples were loaded onto 8 or 10% polyacrylamide gel, transferred to PVDF membrane by using the semi-dry method. Blocking and antibody reactions were done in blocking buffer containing 5% skim milk (Wako, Osaka, Japan) in Tris-buffered saline containing 0.05% Tween 20 (TBS-T). An anti-β-catenin (1:1000, Cell Signaling Technology, Danvers, MA), anti-Histone H3 (1:1000, Cell Signaling Technology), anti-phosphorylated STAT3 (1:1000, Cell Signaling Technology), and HRP-conjugated anti-GAPDH antibody (1:5000, Wako, Osaka, Japan) were used.

Genetic alteration and gene expression in human cancer cases. Genetic alterations and gene expression of *MMP9* were analyzed in whole data (11,1117 samples, 31 types of cancer) available in the TCGA database using cBioPortal version 1/9/2019.

Statistics. Data were expressed as the means ± SD unless otherwise specified. Statistical significance was calculated using GraphPad Prism (La Jolla, CA). Three or more mean values were compared using one-way analysis of variance with the pairwise comparison by the Dunnett's method, while comparisons of 2 were done with an unpaired Student's t-test. $P<0.05$ was considered to indicate statistical significance.

Results
The promoter activity and expression of *Mmp9* were increased in high-metastatic colon cancer cells.

We first conceptualized to establish a novel, convenient reporter system that is useful for evaluation of cancer abilities of tumorigenesis and invasion *in vitro* and *in vivo* (Fig. 1A). For this concept, we combined *Mmp9* promoter-reporter assay and 3D tumoroid culture system, which enable us to measure abilities of invasion and tumorigenesis, respectively. For this purpose, we first examined whether mRNA levels and promoter activities of *Mmp9* were different among 3 different cancer cell lines: murine colon cancer cell line Colon26, its high-metastatic subline LuM1, and none-metastatic subline NM11. The

endogenous mRNA level of *Mmp9* in the high-metastatic LuM1 was 2456-fold higher than that in the parental Colon26 and 52-fold higher than that in the non-metastatic NM11 cell (Fig. 1B). This result was consistent with the high expression of *MMP9* in human colon cancer.
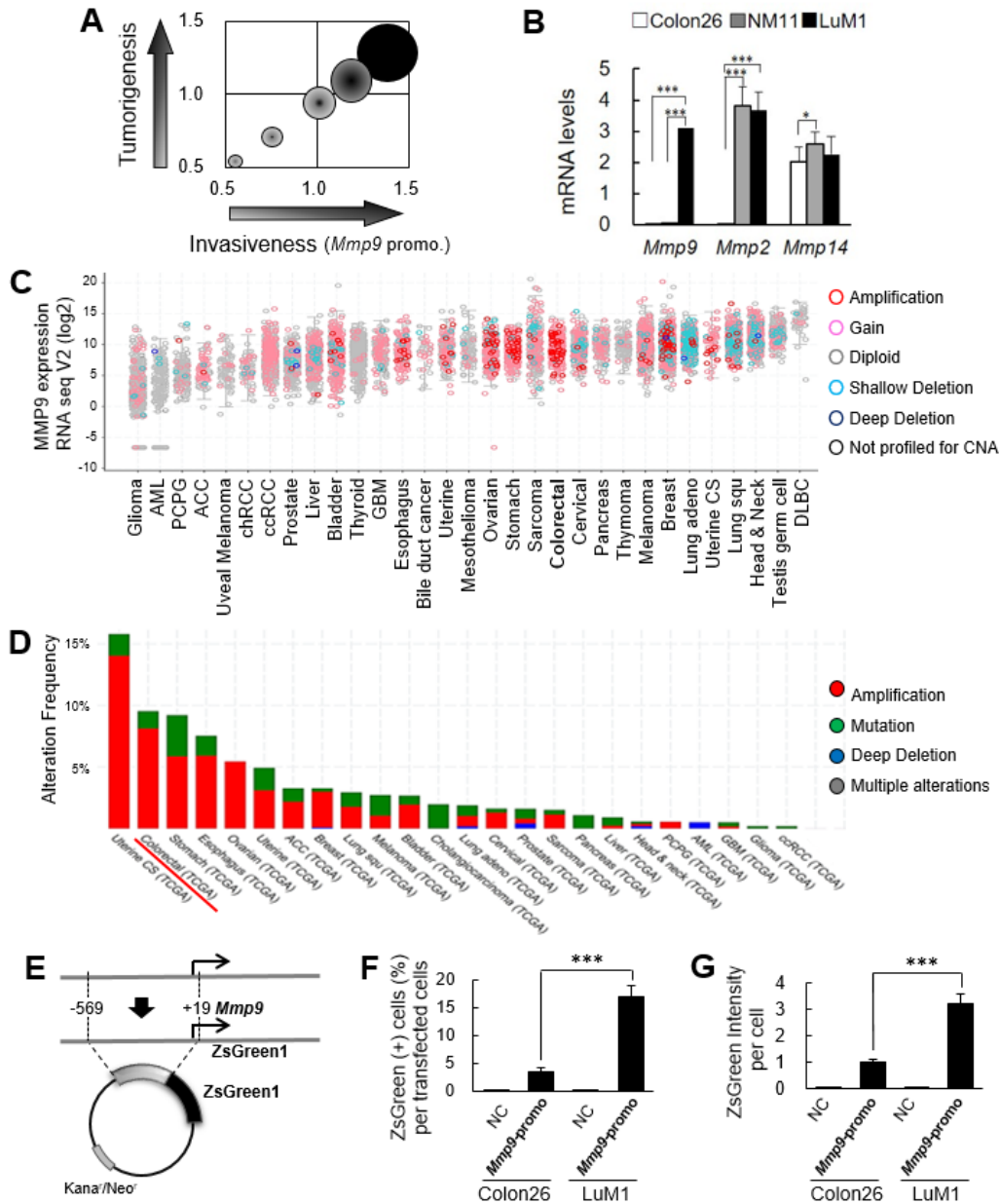

Fig. 1. Increases in the promoter activity and mRNA expression of MMP9 in high-metastatic colon cancer cells. (A) A conceptual scheme showing a novel reporter system that simultaneously evaluates organoid/tumoroid development and invasiveness. (B) mRNA levels of *Mmp9, Mmp2* and *Mmp14* genes in LuM1, NM11, and Colon26 cells. The mRNA levels relative to β-actin mRNA level were shown. Mean ± SD, ***P<0.0001, *P<0.005, n=4. (C, D) mRNA expression and genetic alteration of *MMP9* in various cancer cases. Whole data in the TCGA database was analyzed using cBioPortal. (C) *MMP9* mRNA expression (log$_2$)

in various cancer cases were plotted with the genetic alterations. (D) Alteration frequency of *MMP9* gene in various types of cancers. Twenty four types of cancers with alteration of *MMP9* were aligned. (E) A scheme of the ZsGreen fluorescent reporter construct driven by the *Mmp9* promoter. A 588-bp cDNA fragment of the *Mmp9* promoter region (-569 to +19) was inserted into a pZsGreen1-1 vector. (E, F) The *Mmp9* promoter activities different between LuM1 and Colon26. Transient transfection was carried out. The data were normalized with transfection efficiencies to each cell line using pCMV-GFP. (F) The rate of *Mmp9* promoter-active cells per well. Mean ± SD, n=4. ***P<0.0001. (G) Relative fluorescence intensities per cell. Non-transfected cells were shown as negative controls (NC). Mean ± SD, n=4. ***P<0.0001.

We next investigated the expression and genetic alteration of human *MMP9* among various types of cancers including colon cancer using cBioPortal. The gain of *MMP9* mRNA expression with genetic amplifications was frequently found in colorectal cancer cases compared with other types of cancer such as gliomas (Fig 1C). Amplification of *MMP9* gene in colorectal cancer was found in 8% of total 640 colorectal cancer cases (Fig 1D). It was thus indicated that *MMP9* is expressed at high levels in human and mouse colon cancer.

To investigate a mechanism underlying the high expression of *MMP9*, we next compared proximal promoter sequences between human and mouse. Of note, binding motifs of TCF/LEF, NF-κB, and GR, as well as a TPA-response element (TRE), were conserved between human and mouse *MMP9* promoter regions (Fig S1). For the establishment of a novel reporter system useful for syngeneic transplantation and metastasis in mice, we cloned cDNA corresponding to the murine *Mmp9* promoter region between -569 and +19, which contains multiple transcription factor-binding sites, into ZsGreen fluorescence reporter plasmid (Fig. 1E). The 588-bp *Mmp9* promoter was activated in 17% of LuM1 cells and 3.5% of Colon26 cells (Fig. 1F) (data were normalized with transfection efficiencies to each line shown in Fig S2), consistent with the different levels of *Mmp9* mRNA between these cell lines. *Mmp9* promoter activity per cell was 3-fold higher in LuM1 population than that in Colon26 population (Fig. 1G, Fig. S2). Interestingly, mRNA levels and the promoter activities of *Mmp9* in LuM1 vs Colon26 were not exactly coincident each other, suggesting that expression of MMP9 in cancer could be regulated at both transcriptional and post-transcriptional levels. These data suggested that a potential regulatory mechanism is underlying the increased transcription of *MMP9* specifically in the high-metastatic colon cancer.

Cloning of fluorescent reporter cells that enable monitoring of activities of MMP9/gelatinase, invasion, and metastasis

Recent studies showed heterogeneity of cancer cells, including CIC/CSC, in a single tumor. We therefore next cloned stable fluorescent cells that exert powerful promoter activities of Mmp9, gelatinolytic activities, invasiveness, and metastatic abilities. LuM1 sublines transfected with the *Mmp9* promoter (designated LuM1/m9) #1 and #4 robustly expressed ZsGreen reporter that was driven by the *Mmp9* promoter compared with either sublines #2, #3 or the parental LuM1 cells (Fig. 2A). Gelatinolytic activities of 90-kDa gelatinase B (Gel. B, MMP9) and 60-kDa gelatinase A (Gel. A, MMP2) were higher in culture supernatants of LuM1/m9 sublines #1 and #4 than that of low-metastatic Colon26 (Fig. 2B).

Gelatinase activity of MMP9 of LuM1/m9 #4 was higher than that of the subline #1 (Fig. 2B, arrow). The LuM1/m9 #4 kept powerful fluorescence even after passages whereas other sublines gradually lost their fluorescence. We therefore next examined whether the LuM1/m9 #4 cells possessed invasion abilities *in vitro*. We detected fluorescence of LuM1/m9 #4 cells invaded through matrix and pore at comparable levels with the non-fluorescent parental LuM1 (Fig. 2C).
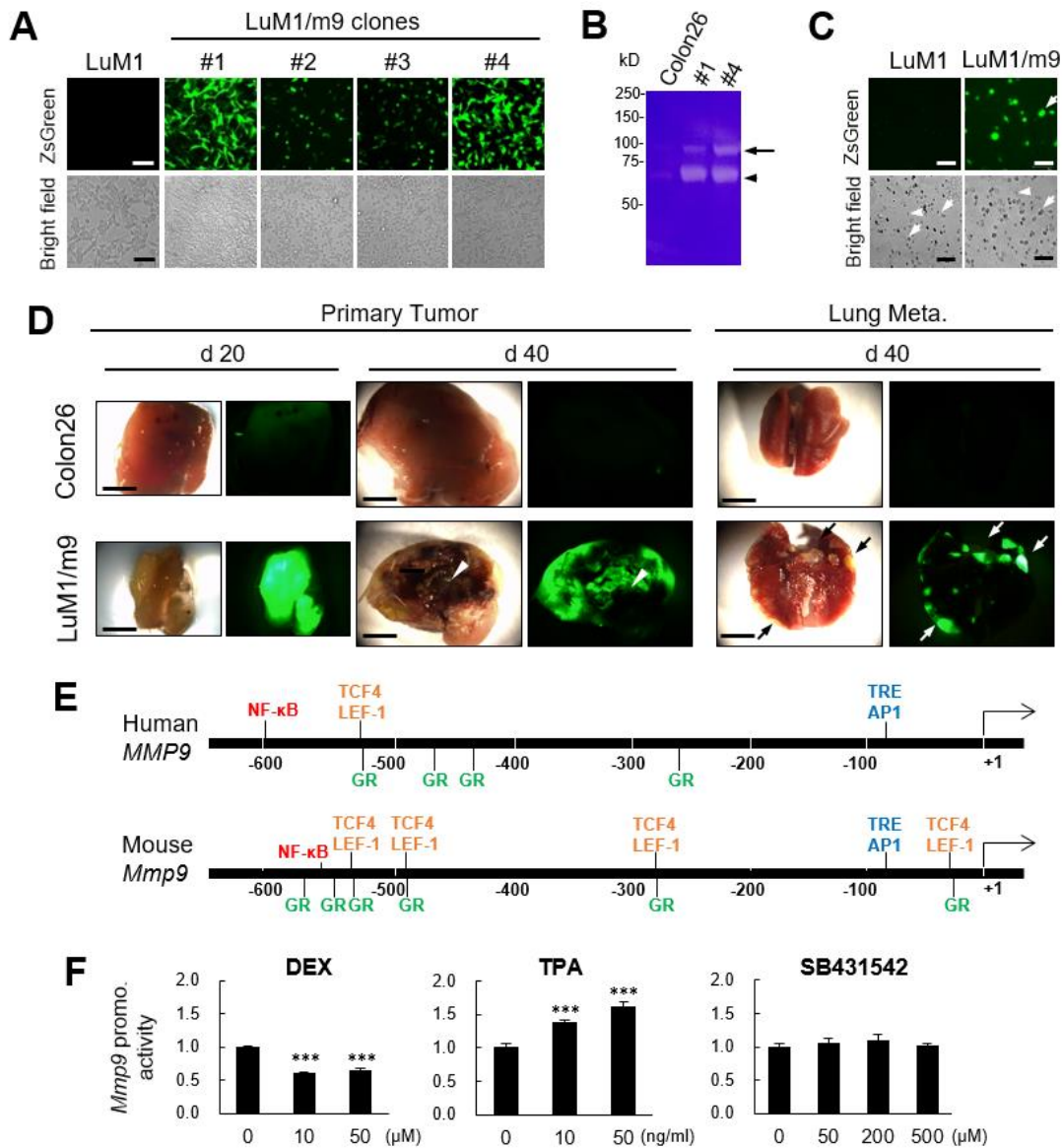

Fig. 2. Stable reporter cells that monitor activities of MMP9/gelatinase, invasion, and metastasis. LuM1 cells were transfected with pZsGreen/Mmp9-promo and stable sublines were established. (A) Representative images of ZsGreen fluorescence of the LuM1/m9 clones #1, #2, #3, and #4. LuM1 was used as non-fluorescent negative control. Scale bars, 100 μm. (B) Gelatinase activities of LuM1/m9 clones #1 and #4 and Colon26. An arrow indicates 90-kD gelatinase B / MMP9. An arrowhead indicates 60-kD gelatinase A / MMP2. (C) *In vitro* invasion of LuM1/m9 #4 was visualized by the fluorescence reporter. Arrows

indicate invaded cells. Arrowheads indicate pores in chambers. Scale bars, 100 μm. (D) Primary and secondary tumors with reporter fluorescence after subcutaneous injection of LuM1/m9 #4. LuM1/m9 #4 and Colon26 cells were subcutaneously injected to side abdominal walls of mice. Subcutaneous tumors and metastatic lung lesions were prepared at day 20 and 40 after the injection. Representative fluorescent images (right images in each pair) and stereomicroscopic images (left images in each pair) of subcutaneous tumors at day 20 (left) and day 40 (center) and metastatic lungs at day 40 (right). Arrows indicate metastatic tumor nodules on the lung. Arrowheads indicate necrotic lesions. Scale bars, 5 mm. (E) Mapping of transcription factor binding sites in the proximal promoter regions of *MMP9* genes in human and mouse. (F) Effects of TPA, DEX, and SB431542 on the *Mmp9* promoter activities of LuM1/m9 reporter cells. LuM1/m9 were cultured in the presence or absence of each drug for 24 h. TPA (10 or 50 ng/ml), DEX (10 or 50 μM), and SB431542 (50, 200 or 500 μM) were used. The fluorescence intensity of ZsGreen was evaluated by ArrayScan^{TM} HCS system. *Mmp9* promoter activities were evaluated by the average of fluorescence intensities per μm^2 of all cells in a well after drug treatment. The values were shown the ratio to non-treated control group. Mean ± SD, n=3-4. **$P<0.01$, ***$P<0.001$ as compared with the group of the absence of each drug.

We next examined whether the LuM1/m9 #4 could have abilities of tumorigenesis and metastasis with detectable reporter fluorescence *in vivo* using syngeneic transplant experiments. Subcutaneous primary tumors at day 20 and day 40 as well as lung metastatic secondary tumors at day 40 showed powerful ZsGreen fluorescence. The tumor at day 20 was filled with ZsGreen-positive live cells (Fig. 2D, bottom left). In contrast, Non-fluorescent "necrotic" area was found in the tumor at day 40 (Fig. 2D, bottom center). Lung metastatic secondary tumor nodules were found with powerful fluorescence at day 40 post-injection period (Fig. 2D bottom right). We also examined tumors formed by the injection of non-fluorescent Colon26 cells as a negative control, which enabled confirmation of LuM1/m9 tumor fluorescence positivity derived from the *Mmp9* promoter-driven reporter gene activation.

Thus, we established a novel fluorescent reporter system for monitoring invasiveness, tumor growth, and metastasis.

Regulation of the *Mmp9* promoter by DEX and TPA

It was suggested that the MMP9 high expression and its powerful promoter activity are biomarkers of cancer activities in terms of invasiveness and metastatic potential. We therefore hypothesized that regulatory signaling for the *Mmp9* promoter plays a key role in controlling cancer activities. By the promoter analysis, we found that many transcription factor-binding sites were conserved between the proximal promoter sequences in human and mouse, including GR, NF-κB, and AP1, whose binding site was shown to be a TPA-response element (TRE) (Fig 2E). To examine whether NF-κB and GR signaling and TPA regulate the *Mmp9* promoter, we investigated whether TPA and DEX could alter the *Mmp9* promoter activity in the metastatic reporter cells. We used these materials because DEX is a type of corticosteroids that antagonize GR and used as a steroidal anti-inflammatory drug (38) and TPA is a carcinogen that activates *MMP9* gene via activation of multiple signaling

pathways including NF-κB, Raf/MEK/ERK, p38 MAPK, and RAC (46, 47). DEX significantly decreased the activity of the *Mmp9* promoter to approximately 60 % of the control at the concentrations of 10 μM and 50 μM (Fig. 2F, left). On the other hand, TPA significantly increased the activity of the *Mmp9* promoter in the metastatic cells at concentrations of 10 and 50 ng/ml (Fig. 2F, center). We also examined TGFβ receptor inhibitor SB431542 as a negative control, since no SMAD binding sequence was found in the *Mmp9* promoter region. As expected, SB431542 did not alter the promoter activity (Fig. 2F, right).

These results indicated that GR and NF-κB signaling are involved in *Mmp9* expression in metastatic cancer cells, although another signal might also regulate the *Mmp9* promoter as investigated in the following studies.

β-catenin stability and 3D tumor growth enhance the *Mmp9* promoter activity.

The intra-tumoral milieu is being hypoxic when enlarged and thus hypoxia-inducible factor 1 (HIF1) activate *MMP* genes (48-50). In addition, we recently reported that both hypoxic organoid/tumoroid formation and stemness-enhancing medium mTeSR1 increased stem-cell properties (1, 2). The mTeSR1 medium contains LiCl that activate β-catenin signaling by inhibiting GSK3 (41, 51). Therefore, we hypothesized that Wnt/β-catenin signaling for stem cell renewal could also mediate high-expression of MMP9 during tumorigenesis. To test this hypothesis, we examined whether the 3D tumoroid-inducing milieu and LiCl could increase tumorigenesis as well as the *Mmp9* promoter activity. LuM1/m9 #4 were seeded onto 2D culture plate or 3D NCP, and cultured in RPMI 1640 with 10% FBS (serum) or mTeSR1 (stem). After 2 days of incubation, the size of tumoroid and the *Mmp9* promoter-driven reporter fluorescence were measured using the ArrayScan™ HCS system. Tumoroids were enlarged with fluorescence in 3D tumoroid-inducing NCPs (3D-serum) and mTeSR1 medium (2D-stem) and furthermore enlarged by their combination (3D-stem) (Fig. 3 A and B). Simultaneously, *Mmp9* promoter activity was increased in 3D tumoroid-inducing culture (3D-serum) and mTeSR1 medium (2D-stem) and further increased by their combination (3D-stem) (Fig. 3C).

We next examined the scatter plot analysis of every single aggregate in terms of their size (vertical axis) and *Mmp9* promoter activities (horizontal axis). The 3D culture on NCP (3D-serum) markedly increased *Mmp9* promoter activity as well as a tumoroid formation (Fig. 3D, compare graphs on the left and center). The add-on of mTeSR1 medium to the 3D culture system (3D-stem) markedly increased the size of tumoroid (Fig. 3D, compare graphs on the right and center), consistent with the data shown in Fig. 3 A-C. Thus, these data suggested a synergistic effect of 3D culture and stemness-enhancing signaling on the tumoroid formation. As the mTeSR1 medium contains LiCl, a stimulator of β-catenin signaling, we next examined β-catenin in the tumoroids and effects of LiCl on cell-aggregation and *Mmp9* promoter activities. β-catenin was found in both nuclear and cytoplasmic fractions of the 3D-stem tumoroids of the LuM1/m9 cells, whereas this factor was not detected in the 2D-serum culture condition (Fig. 3E), suggesting that LiCl in mTeSR1 medium might contribute to the stabilization of β-catenin through inhibition of GSK3β, an inhibitory factor of β-catenin (Fig. 3F).
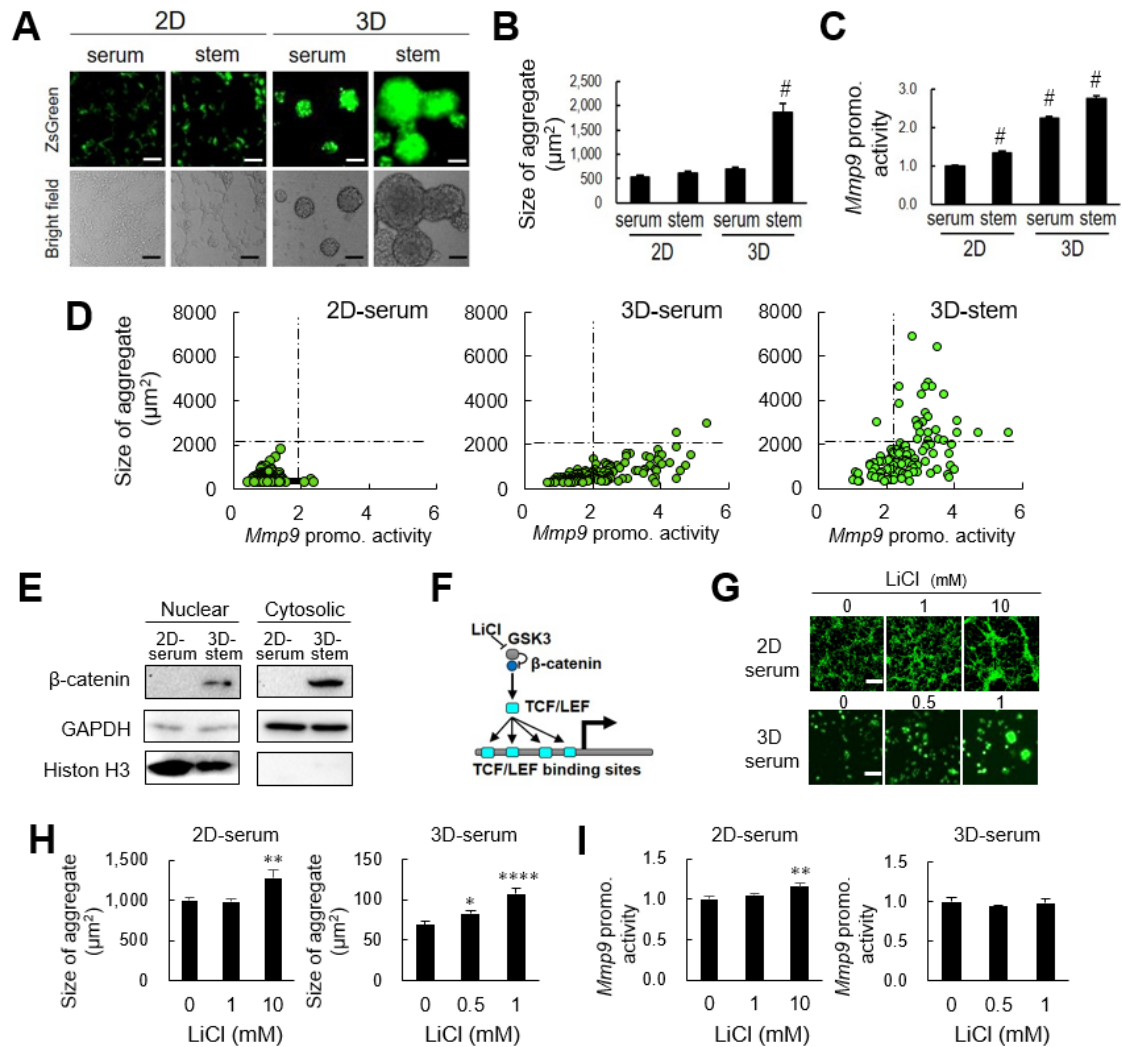
11

Fig. 3. The stability of β-catenin and 3D tumor growth enhanced the *Mmp9* promoter activity. (A-E) The LuM1/m9 #4 were cultured in 2D serum-containing condition (2D-serum), 2D stem-cell medium condition (2D-stem), 3D serum-containing condition (3D-serum) or 3D stem-cell medium condition (3D-stem) for 2 days. (A) Representative images of cells/tumoroids with reporter fluorescence (top) and bright fields (bottom). (B) The average size of the cell aggregates. Mean ± SD, n=4. #P<0.0001, vs 2D-serum. (C) The average of *Mmp9* promoter activities of all cell-aggregates/tumoroids in a well. The values were shown the ratio to 2D-serum group. Mean ± SD, n=4. #P<0.0001, vs 2D serum. (D) Scatter plot analysis of all cell-aggregates/tumoroids in the wells. Cell aggregates/tumoroids were plotted according to their size (horizontal axis) and fluorescence intensities per μm^2 in each cell-aggregate/tumoroid (vertical axis). 2D-serum, n=276. 3D-serum, n=160. 3D-stem, n=108. (E) Western blot analysis of β-catenin in nuclear and cytoplasmic localization. Histone H3 was blotted as a marker of nuclei. GAPDH was blotted as a marker of cytoplasm. (F) A conceptual scheme of the reporter assay that evaluates β-catenin/TCF/MMP9 axis. LiCl was used as an activator of β-catenin-TCF/LEF signaling through inhibition of GSK3β. (G to I) Effect of LiCl on the LuM1/m9 reporter cells in 2D and 3D conditions. In the 2D condition, after pre-cultured in RPMI1640 with 10% serum for 2 days, cells were cultured with LiCl at

12

a final concentration 1 or 10 mM in RPMI1640 with 2% serum for 2 days. In the 3D condition, cells were cultured in the presence or absence of LiCl at final concentration 0.5 or 1 mM in RPMI1640 with 2% serum for 3 days. A detailed protocol was drawn in Fig. S2 A and I. (G) Representative fluorescent reporter images of cell-aggregates. Scale bars, 100 μm. (H) Size of LuM1/m9 cell-aggregates. Fluorescent areas greater than 300 μm² were deemed to be cell-aggregates in 2D condition. All cell-aggregates were measured in 3D condition. Mean ± SD, n=3, **$P<0.01$, ***$P<0.001$ vs non-treated control group. (I) *Mmp9* promoter activities per cell-aggregates. Mean ± SD, n=3. ***$P<0.001$, vs non-treated control group.

It has been shown that after stabilization, β-catenin translocate to nuclei, where this factor binds to TCF/LEF (51), whose consensus binding sequences were found in the *Mmp9* promoter sequence (Fig. 2E, 3F). The size of cell-aggregates was increased by LiCl in either 2D-serum or 3D-serum conditions (Fig. 3 G, H, Fig S3), suggesting that stabilized β-catenin/TCF complex might activate its target cyclin D gene that promotes cell proliferation. The *Mmp9* promoter activity was increased by the administration of LiCl in the 2D-serum condition (Fig 3I), although the activity was not altered in the 3D-stem tumoroid (Fig. S3), suggesting that the *Mmp9* promoter might be occupied by hypoxia-HIF1 signaling in such large tumoroids.

These findings suggested that stabilized β-catenin/MMP9 regulatory axis was activated during tumor growth (while intra-tumoral hypoxia-MMP9 regulatory axis could be simultaneously activated when the tumor was enlarged). It was also indicated that the combination of NCP-based 3D culture and mTeSR1 stemness-enhancing medium or LiCl is useful for the development of tumoroid studies.

ART inhibited tumorigenesis and the *Mmp9* promoter of metastatic colon cancer cells *in vitro*.

Our reporter system has been demonstrated to be useful for monitoring cancer invasiveness, metastasis, 3D tumorigenesis *in vitro*, and key signalings such as NF-κB and Wnt/β-catenin. Therefore, it is supposed that this reporter system could also be suitable and useful for drug screening with an advantage of 3D tumoroid formation within the culture medium. We examined the effects of ART, 5-FU, and HC on *in vitro* tumorigenesis using this 3D reporter system as a pilot study. LuM1/m9 #4 were seeded and simultaneously treated with 5-FU, HC or ART within mTeSR1 stem-cell medium in NCPs. After 3 days of incubation, the size of tumoroid and the *Mmp9* promoter-driven reporter fluorescence were measured using the ArrayScan™ HCS system (Fig. 4A). The average size of organoid and the average activity of the *Mmp9* promoter in tumoroid were depicted as a scatter plot. 5-FU significantly inhibited tumorigenesis to approximately 50 % of the control but did not decrease the *Mmp9* promoter activity at a concentration of 10 μM (Fig. 4B, bottom right; Fig. S4). ART significantly inhibited both the *Mmp9* promoter activity and tumorigenesis to approx. 85% and 40 % of the control, respectively, at a concentration of 20 μM (Fig. 4B, bottom left; Fig S4). HC (2 μM) inhibited the *Mmp9* promoter activity to approximately 20% of the control but did not inhibit *in vitro* tumorigenesis (Fig. 4B, top left; Fig S4). Lower concentrations of ART (2 or 4 μM) and 5-FU (1 μM) did not alter either the size of tumoroids or the *Mmp9* promoter activities (Fig. S4).
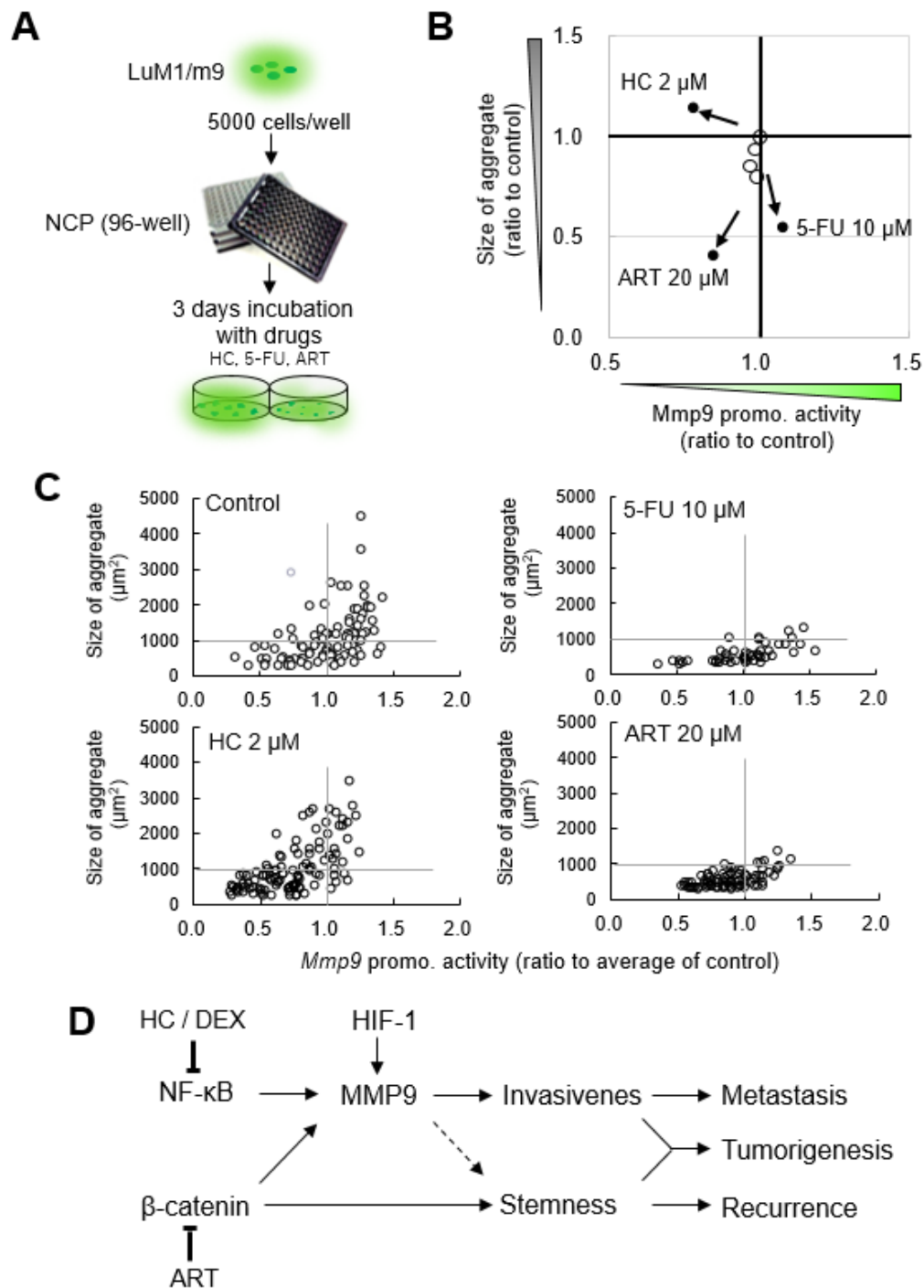
Fig. 4. Artesunate inhibited tumorigenesis and the *Mmp9* promoter of metastatic colon cancer cells *in vitro*. (A) A conceptual schema of drug screening for dual inhibitors of tumorigenesis and invasiveness using the combination of tumoroid culture and LuM1/m9 #4 reporter cells. Hydrocortisone (HC), 5-fluorouracil (5-FU), and artesunate (ART) were used in this pilot study. To investigate the effects of HC, 5-FU, and ART, cells were seeded at a concentration of 5×10^3 cells/well in a 96-well NCP and cultured in mTeSR1 stem-cell medium for 3 days with drugs. (B) Scatter plot analysis of drug effects on tumorigenesis and the Mmp9 promoter activities. The horizontal axis was plotted with the average of *Mmp9*

promoter activities in tumoroids (ratio to control) per well. The vertical axis was plotted the average size of tumoroids (ratio to control) per well. Arrows indicate 2 μM HC, 20 μM ART, and 10 μM 5-FU. The other plots indicate 2 or 4 μM ART, 1 μM 5-FU or non-treated control (plotted at 1.0 and 1.0). Data with statistics were shown in Fig. S3. (C) Scatter plot analysis of all tumoroids in each well. All tumoroids were plotted according to their size (horizontal axis) and the fluorescence intensities per pixel ($=\mu m^2$) (vertical axis). (D) A schematic summary. The novel fluorescent reporter system of the *Mmp9* promoter in a combination with 3D tumoroid culture is useful for studies of tumorigenesis, invasiveness, metastasis, signaling pathways, pharmacology, and drug discovery. MMP9 is an essential factor in cancer invasion and metastasis (9). MMP9 gene is activated by multiple signaling such as Wnt/β-catenin/TCF signaling (early stage), NF-κB signaling, and hypoxia-HIF1 signaling (late stage). ART decrease tumorigenesis and MMP expression via inhibition of Wnt/β-catenin signaling. Both glucocorticoid HC and corticosteroid DEX inhibited the *Mmp9* promoter potentially via inhibiting GR/NF-κB complex.

We next depicted scatter plots of all cell-aggregates per well in terms of their size (vertical axis) and *Mmp9* promoter activities (horizontal axis). It was shown that 5-FU and ART inhibited *in vitro* tumorigenesis compared with control or HC (Fig. 4C). HC and ART tended to attenuate the *Mmp9* promoter activities compared with the control or 5-FU, although tumoroids with high *Mmp9* promoter activity were still present even after the treatment with HC or ART (Fig. 4C). Since many STAT binding sites were found in the *Mmp9* promoter region as shown in Fig S1, we examined STAT inhibitor AG490 and detection of phosphorylated STAT3 (p-STAT), which is often active in stem cells. However, AG490 altered neither the *in vitro* tumorigenesis nor the *Mmp9* promoter activity. The p-STAT3 was barely detectable in the 2D-serum and the 3D-stem conditions (Fig. S5).

Thus, these findings indicate that (i) ART inhibit tumorigenesis and *Mmp9* promoter potentially through inhibition of β-catenin, (ii) HC inhibits *Mmp9* promoter by a potential mechanism underlying HC/DEX-dependent repression of GR/NF-κB complex, (iii) 5-FU inhibit tumorigenesis.

Discussion

Our studies established a novel reporter system that enables to monitor tumorigenesis *in vivo* and *in vitro*, metastasis, invasiveness, and is useful for studies of signaling, transcription, and drugs that alter promoter activity of MMP9, which is one of the key biomarker as well as a causal factor in cancer progression. We showed that the 588-bp *Mmp9* promoter-driven reporter cells (LuM1/m9) were profoundly gelatinolytic and invasive (Fig. 1, 2). This *Mmp9* promoter-reporter monitored cancer cells at both primary and secondary tumors *in vivo* (Fig. 2D). The quantitative analysis of the tumoroid size and the reporter activities enabled efficient pharmaceutical studies (Fig. 3, 4). Although numerous factors and signaling pathways have been shown to involve CIC/CSC (2, 25, 52-56), to elucidate key factors that could promote tumoroid growth with enhanced stemness and increased *Mmp9* promoter activity, we analyzed the *MMP9* promoter sequence and then found that a TCF/LEF-binding site was conserved between human and mouse (Fig. 2E). It has been shown that Wnt/β-catenin/TCF signaling is essential for self-renewal of CIC/CSC

(29). Our present study showed that β-catenin was stabilized in the 3D-stem tumoroid culture condition, presumably through inhibition of GSK3β by LiCl supplemented in the mTeSR1. Such stabilization of β-catenin could trigger nuclear translocation of this factor (Fig. 3E). To elucidate whether the β-catenin-TCF/LEF signal is crucial for activation of the *Mmp9* promoter, we used LiCl, which can activate β-catenin-TCF/LEF signaling. Indeed, LiCl exposure increased *Mmp9* promoter activity as well as cell aggregates. Such effects of LiCl on the growth of cell-aggregates and on activation of the *Mmp9* promoter were observed in early stages of tumorigenesis, in which β-catenin/TCF might activate its target gene cyclin D1 (33). Thus, our data touch upon the Wnt/β-catenin regulation of *MMP9* in colon cancer. This is consistent with a recent report that Wnt3a expression is associated with *MMP9* expression in primary tumor and metastatic site in recurrent or stage IV colorectal cancer (18). Another study also reported the β-catenin regulation of *MMP9* in melanoma using a β-catenin inhibitor lycorine (57). However, in the present study, LiCl was ineffective when the tumoroid grew larger, which mimic later stage of tumors. The interior of tumors is hypoxic, in which HIF1 activates *MMP9* gene and other oncogenes (1, 2, 52, 58-61). Therefore, targeting Wnt/β-catenin signaling might be effective only at the early stage of tumorigenesis, whereas targeting hypoxia-HIF1 signaling might be effective for enlarged hypoxic tumors at the later stage. Regardless of the activities of β-catenin/TCF signaling or hypoxia-HIF1 signaling, we showed that siRNA-targeted depletion of MMP9 and MMP3 was effective to inhibit tumorigenesis and metastasis (10). Moreover, not only extracellular proteolytic MMPs but also intracellular MMPs could contribute to cancer transcriptional regulation and migration (10, 20-22).

Our studies also indicated that 5-FU was effective to decrease tumorigenesis of the MMP9 high colon cancer cells. 5-FU resistance has been shown in colon cancer and its mechanism is still unclear (62). Nevertheless, a recent study reported that overexpression of MMP9 and Rab1B predicts poor survival and good response to chemotherapy in patients with colorectal cancer (17). This report is consistent with our finding that 5-FU was effective to decrease tumorigenesis of the MMP9 high colon cancer cells (Fig 4). In clinical cases, 5-FU has been applied mostly in combination with other substances (63). Therefore, a combination of therapeutics that were found to be effective may solve resistance and recurrence of cancer. Our pilot study also revealed some effectiveness of ART on *Mmp9* promoter activity and tumorigenesis (Fig 4), in which β-catenin was stabilized. It has been shown that the anti-cancer activity of ART correlated with the inhibition of hyperactive Wnt/β-catenin signaling pathway (64, 65). Moreover, it was shown that ART inhibited the expression of several MMPs, including MMP2 and MMP7 mRNA/proteins (66). These studies were consistent with our findings that ART inhibited both the *Mmp9* promoter and *in vitro* tumor formation, in which β-catenin-TCF/LEF signaling was active. Therefore, ART is useful as an anti-cancer medication that inhibits tumorigenesis, invasiveness, recurrence, and resistance of cancer through targeting Wnt/β-catenin/MMPs regulatory axis.

Due to practical and ethical limitations in human experimentation, animal models have been essential in cancer research. However, the average rate of successful translation from animal models to clinical cancer trials is less than 8% (67). Animal models can provide a key source of in vivo information, but alternative translational methods have emerged that may eventually replace the connection between in vitro studies and clinical applications.

Human tissue models in cancer research, including patient-derived xenograft (PDX) mice, are widely used to address questions in cancer research (68). The latest animal models of human colon cancer have opened up new doors for continuing cancer research for not only understanding the colon cancer pathogenesis but also aid in the development of newer chemotherapeutic drugs as they mimic the human disease closely (69). However, each reported model has some limitations. A limitation using human cancer cells is that researchers ought to transplant the human-derived cancer cells to immunodeficient mice such as nude mice or severe combined immunodeficient (SCID) mice, in which studies on tumor immunology are limited. Our reporter system was established using mouse metastatic colon cancer cells that are useful for syngeneic transplantation to immunologically normal mice, in which researchers could analyze tumor milieu and immunology. Moreover, we have developed the 3D tumoroid system using mouse-derived cancer cells as well as human-derived cells (1, 2). Growing cells as 3D models are more analogous to their existence in vivo, for example, akin to a tumor, and is able to be co-cultured with other cells and cellular components that naturally occur in their milieu may be more clinically relevant (9). Therefore, the LuM1/M9 reporter system established with the BALB/c mouse-derived cancer cells in the present study could be useful for 3D tumoroid model cocultured with other types of cells such as immune cells and for syngeneic transplantation to investigate tumor microenvironment and tumor immunology.

In conclusion, this novel fluorescent reporter system for dual monitoring of tumorigenesis and the *Mmp9* promoter activity in vitro and in vivo is useful for studies of invasiveness, metastasis, signaling pathways, pharmacology, and drug discovery. It was also demonstrated that ART inhibited *in vitro* 3D tumorigenesis and *Mmp9* promoter activity, potentially via inhibiting Wnt/β-catenin signaling.

References

1. Namba, Y., Sogawa, C., Okusha, Y., Kawai, H., Itagaki, M., Ono, K., Murakami, J., Aoyama, E., Ohyama, K., Asaumi, J.I., Takigawa, M., Okamoto, K., Calderwood, S.K., Kozaki, K.I., andEguchi, T. Depletion of Lipid Efflux Pump ABCG1 Triggers the Intracellular Accumulation of Extracellular Vesicles and Reduces Aggregation and Tumorigenesis of Metastatic Cancer Cells. Front Oncol **8**, 376, 2018.

2. Eguchi, T., Sogawa, C., Okusha, Y., Uchibe, K., Iinuma, R., Ono, K., Nakano, K., Murakami, J., Itoh, M., Arai, K., Fujiwara, T., Namba, Y., Murata, Y., Ohyama, K., Shimomura, M., Okamura, H., Takigawa, M., Nakatsura, T., Kozaki, K.I., Okamoto, K., andCalderwood, S.K. Organoids with cancer stem cell-like properties secrete exosomes and HSP90 in a 3D nanoenvironment. PLoS One **13**, e0191109, 2018.

3. Ishiguro, T., Ohata, H., Sato, A., Yamawaki, K., Enomoto, T., andOkamoto, K. Tumor-derived spheroids: Relevance to cancer stem cells and clinical applications. Cancer Sci **108**, 283, 2017.

4. Takai, A., Fako, V., Dang, H., Forgues, M., Yu, Z., Budhu, A., andWang, X.W. Three-dimensional Organotypic Culture Models of Human Hepatocellular Carcinoma. Sci Rep **6**, 21174, 2016.

5. van de Wetering, M., Francies, H.E., Francis, J.M., Bounova, G., Iorio, F., Pronk, A., van Houdt, W., van Gorp, J., Taylor-Weiner, A., Kester, L., McLaren-Douglas, A., Blokker, J., Jaksani, S., Bartfeld, S., Volckman, R., van Sluis, P., Li, V.S., Seepo, S., Sekhar Pedamallu, C., Cibulskis, K., Carter, S.L., McKenna, A., Lawrence, M.S., Lichtenstein, L., Stewart, C., Koster, J., Versteeg, R., van Oudenaarden, A., Saez-Rodriguez, J., Vries, R.G., Getz, G., Wessels, L., Stratton, M.R., McDermott, U., Meyerson, M., Garnett, M.J., andClevers, H.

Prospective derivation of a living organoid biobank of colorectal cancer patients. Cell **161**, 933, 2015.

6.   Boj, S.F., Hwang, C.I., Baker, L.A., Chio, II, Engle, D.D., Corbo, V., Jager, M., Ponz-Sarvise, M., Tiriac, H., Spector, M.S., Gracanin, A., Oni, T., Yu, K.H., van Boxtel, R., Huch, M., Rivera, K.D., Wilson, J.P., Feigin, M.E., Ohlund, D., Handly-Santana, A., Ardito-Abraham, C.M., Ludwig, M., Elyada, E., Alagesan, B., Biffi, G., Yordanov, G.N., Delcuze, B., Creighton, B., Wright, K., Park, Y., Morsink, F.H., Molenaar, I.Q., Borel Rinkes, I.H., Cuppen, E., Hao, Y., Jin, Y., Nijman, I.J., Iacobuzio-Donahue, C., Leach, S.D., Pappin, D.J., Hammell, M., Klimstra, D.S., Basturk, O., Hruban, R.H., Offerhaus, G.J., Vries, R.G., Clevers, H., andTuveson, D.A. Organoid models of human and mouse ductal pancreatic cancer. Cell **160**, 324, 2015.

7.   Karthaus, W.R., Iaquinta, P.J., Drost, J., Gracanin, A., van Boxtel, R., Wongvipat, J., Dowling, C.M., Gao, D., Begthel, H., Sachs, N., Vries, R.G., Cuppen, E., Chen, Y., Sawyers, C.L., andClevers, H.C. Identification of multipotent luminal progenitor cells in human prostate organoid cultures. Cell **159**, 163, 2014.

8.   Tauro, B.J., Greening, D.W., Mathias, R.A., Mathivanan, S., Ji, H., andSimpson, R.J. Two distinct populations of exosomes are released from LIM1863 colon carcinoma cell-derived organoids. Mol Cell Proteomics **12**, 587, 2013.

9.   Breslin, S., andO'Driscoll, L. Three-dimensional cell culture: the missing link in drug discovery. Drug Discov Today **18**, 240, 2013.

10.   Okusha, Y., Eguchi, T., Sogawa, C., Okui, T., Nakano, K., Okamoto, K., andKozaki, K.I. The intranuclear PEX domain of MMP involves proliferation, migration, and metastasis of aggressive adenocarcinoma cells. J Cell Biochem **119**, 7363, 2018.

11.   Reggiani, F., Labanca, V., Mancuso, P., Rabascio, C., Talarico, G., Orecchioni, S., Manconi, A., andBertolini, F. Adipose Progenitor Cell Secretion of GM-CSF and MMP9 Promotes a Stromal and Immunological Microenvironment That Supports Breast Cancer Progression. Cancer Res **77**, 5169, 2017.

12.   Kessenbrock, K., Dijkgraaf, G.J., Lawson, D.A., Littlepage, L.E., Shahi, P., Pieper, U., andWerb, Z. A role for matrix metalloproteinases in regulating mammary stem cell function via the Wnt signaling pathway. Cell Stem Cell **13**, 300, 2013.

13.   Vandenbroucke, R.E., andLibert, C. Is there new hope for therapeutic matrix metalloproteinase inhibition? Nat Rev Drug Discov **13**, 904, 2014.

14.   Sato H, Takino T, Okada Y, Cao J, Shinagawa A, Yamamoto E, andSeiki, M. A matrix metalloproteinase expressed on the surface of invasive tumour cells. Nature **370**, 61, 1994.

15.   Schlage, P., Kockmann, T., Sabino, F., Kizhakkedathu, J.N., andAuf dem Keller, U. Matrix Metalloproteinase 10 Degradomics in Keratinocytes and Epidermal Tissue Identifies Bioactive Substrates With Pleiotropic Functions. Mol Cell Proteomics **14**, 3234, 2015.

16.   Hashimoto, G., Inoki, I., Fujii, Y., Aoki, T., Ikeda, E., andOkada, Y. Matrix metalloproteinases cleave connective tissue growth factor and reactivate angiogenic activity of vascular endothelial growth factor 165. J Biol Chem **277**, 36288, 2002.

17.   Yang, X.Z., Cui, S.Z., Zeng, L.S., Cheng, T.T., Li, X.X., Chi, J., Wang, R., Zheng, X.F., andWang, H.Y. Overexpression of Rab1B and MMP9 predicts poor survival and good response to chemotherapy in patients with colorectal cancer. Aging (Albany NY) **9**, 914, 2017.

18.   Lee, M.A., Park, J.H., Rhyu, S.Y., Oh, S.T., Kang, W.K., andKim, H.N. Wnt3a expression is associated with MMP-9 expression in primary tumor and metastatic site in recurrent or stage IV colorectal cancer. BMC Cancer **14**, 125, 2014.

19.   Newell, K.J., Witty, J.P., Rodgers, W.H., andMatrisian, L.M. Expression and localization of matrix-degrading metalloproteinases during colorectal tumorigenesis. Mol Carcinog **10**, 199, 1994.

20.   Eguchi, T., Calderwood, S.K., Takigawa, M., Kubota, S., andKozaki, K.I. Intracellular MMP3 Promotes HSP Gene Expression in Collaboration With Chromobox Proteins. J Cell Biochem **118**, 43, 2017.

21.   Eguchi, T., Kubota, S., Kawata K., Mukudai Y., Uehara J., Ohgawara T., Ibaragi S, Sasaki A., Kuboki, T., andTakigawa, M. Novel Transcriptional Regulation of CCN2/CTGF by Nuclear Translocation of MMP3. Dordrecht, Nertherlands: Springer; 2010.

22.   Eguchi, T., Kubota, S., Kawata, K., Mukudai, Y., Uehara, J., Ohgawara, T., Ibaragi, S., Sasaki, A., Kuboki, T., andTakigawa, M. Novel transcription-factor-like function of human matrix metalloproteinase 3 regulating the CTGF/CCN2 gene. Mol Cell Biol **28**, 2391, 2008.

23.   Mizushima, H., Wang, X., Miyamoto, S., andMekada, E. Integrin signal masks growth-promotion activity of HB-EGF in monolayer cell cultures. J Cell Sci **122**, 4277, 2009.

24.   Baker, B.M., andChen, C.S. Deconstructing the third dimension: how 3D culture microenvironments alter cellular cues. J Cell Sci **125**, 3015, 2012.

25.   Arai, K., Eguchi, T., Rahman, M.M., Sakamoto, R., Masuda, N., Nakatsura, T., Calderwood, S.K., Kozaki, K., andItoh, M. A Novel High-Throughput 3D Screening System for EMT Inhibitors: A Pilot Screening Discovered the EMT Inhibitory Activity of CDK2 Inhibitor SU9516. PLoS One **11**, e0162394, 2016.

26.   Shibue, T., andWeinberg, R.A. EMT, CSCs, and drug resistance: the mechanistic link and clinical implications. Nat Rev Clin Oncol **14**, 611, 2017.

27.   Tammela, T., Sanchez-Rivera, F.J., Cetinbas, N.M., Wu, K., Joshi, N.S., Helenius, K., Park, Y., Azimi, R., Kerper, N.R., Wesselhoeft, R.A., Gu, X., Schmidt, L., Cornwall-Brady, M., Yilmaz, O.H., Xue, W., Katajisto, P., Bhutkar, A., andJacks, T. A Wnt-producing niche drives proliferative potential and progression in lung adenocarcinoma. Nature **545**, 355, 2017.

28.   Chou, S.D., Murshid, A., Eguchi, T., Gong, J., andCalderwood, S.K. HSF1 regulation of beta-catenin in mammary cancer cells through control of HuR/elavL1 expression. Oncogene **34**, 2178, 2015.

29.   Woodward, W.A., Chen, M.S., Behbod, F., Alfaro, M.P., Buchholz, T.A., andRosen, J.M. WNT/beta-catenin mediates radiation resistance of mouse mammary progenitor cells. Proc Natl Acad Sci U S A **104**, 618, 2007.

30.   Sugimura, R., He, X.C., Venkatraman, A., Arai, F., Box, A., Semerad, C., Haug, J.S., Peng, L., Zhong, X.B., Suda, T., andLi, L. Noncanonical Wnt signaling maintains hematopoietic stem cells in the niche. Cell **150**, 351, 2012.

31.   Morin, P.J., Sparks, A.B., Korinek, V., Barker, N., Clevers, H., Vogelstein, B., andKinzler, K.W. Activation of beta-catenin-Tcf signaling in colon cancer by mutations in beta-catenin or APC. Science **275**, 1787, 1997.

32.   Gotoh, J., Obata, M., Yoshie, M., Kasai, S., andOgawa, K. Cyclin D1 over-expression correlates with beta-catenin activation, but not with H-ras mutations, and phosphorylation of Akt, GSK3 beta and ERK1/2 in mouse hepatic carcinogenesis. Carcinogenesis **24**, 435, 2003.

33.   Tetsu, O., andMcCormick, F. Beta-catenin regulates expression of cyclin D1 in colon carcinoma cells. Nature **398**, 422, 1999.

34.   Metcalfe, C., andBienz, M. Inhibition of GSK3 by Wnt signalling--two contrasting models. J Cell Sci **124**, 3537, 2011.

35.   Longley, D.B., Harkin, D.P., andJohnston, P.G. 5-fluorouracil: mechanisms of action and clinical strategies. Nat Rev Cancer **3**, 330, 2003.

36.   Efferth, T., Dunstan, H., Sauerbrey, A., Miyachi, H., andChitambar, C.R. The anti-malarial artesunate is also active against cancer. Int J Oncol **18**, 767, 2001.

37. Subedi, A., Futamura, Y., Nishi, M., Ryo, A., Watanabe, N., andOsada, H. High-throughput screening identifies artesunate as selective inhibitor of cancer stemness: Involvement of mitochondrial metabolism. Biochem Biophys Res Commun **477**, 737, 2016.

38. Ray, A., andPrefontaine, K.E. Physical association and functional antagonism between the p65 subunit of transcription factor NF-kappa B and the glucocorticoid receptor. Proc Natl Acad Sci U S A **91**, 752, 1994.

39. Jonat, C., Rahmsdorf, H.J., Park, K.K., Cato, A.C., Gebel, S., Ponta, H., andHerrlich, P. Antitumor promotion and antiinflammation: down-modulation of AP-1 (Fos/Jun) activity by glucocorticoid hormone. Cell **62**, 1189, 1990.

40. Sakata K, Kozaki K, Iida K, Tanaka R, Yamagata S, Utsumi KR, Saga S, Shimizu S, andMatsuyama, M. Establishment and characterization of high- and low-lung-metastatic cell lines derived from murine colon adenocarcinoma 26 tumor line. Jpn J Cancer Res (Cancer Sci) **87**, 78, 1996.

41. Akopian, V., Andrews, P.W., Beil, S., Benvenisty, N., Brehm, J., Christie, M., Ford, A., Fox, V., Gokhale, P.J., Healy, L., Holm, F., Hovatta, O., Knowles, B.B., Ludwig, T.E., McKay, R.D., Miyazaki, T., Nakatsuji, N., Oh, S.K., Pera, M.F., Rossant, J., Stacey, G.N., andSuemori, H. Comparison of defined culture systems for feeder cell free propagation of human embryonic stem cells. In Vitro Cell Dev Biol Anim **46**, 247, 2010.

42. Yoshii, Y., Waki, A., Yoshida, K., Kakezuka, A., Kobayashi, M., Namiki, H., Kuroda, Y., Kiyono, Y., Yoshii, H., Furukawa, T., Asai, T., Okazawa, H., Gelovani, J.G., andFujibayashi, Y. The use of nanoimprinted scaffolds as 3D culture models to facilitate spontaneous tumor cell migration and well-regulated spheroid formation. Biomaterials **32**, 6052, 2011.

43. Eguchi, T., Kubota, S., andTakigawa, M. Promoter Analyses of CCN Genes. Methods Mol Biol **1489**, 177, 2017.

44. Sato, H., Kita, M., andSeiki, M. v-Src activates the expression of 92-kDa type IV collagenase gene through the AP-1 site and the GT box homologous to retinoblastoma control elements. A mechanism regulating gene expression independent of that by inflammatory cytokines. J Biol Chem **268**, 23460, 1993.

45. Ono, K., Eguchi, T., Sogawa, C., Calderwood, S.K., Futagawa, J., Kasai, T., Seno, M., Okamoto, K., Sasaki, A., andKozaki, K.I. HSP-enriched properties of extracellular vesicles involve survival of metastatic oral cancer cells. J Cell Biochem 2018.

46. Kang, J.H., Asai, D., Yamada, S., Toita, R., Oishi, J., Mori, T., Niidome, T., andKatayama, Y. A short peptide is a protein kinase C (PKC) alpha-specific substrate. Proteomics **8**, 2006, 2008.

47. Shin, Y., Yoon, S.H., Choe, E.Y., Cho, S.H., Woo, C.H., Rho, J.Y., andKim, J.H. PMA-induced up-regulation of MMP-9 is regulated by a PKCalpha-NF-kappaB cascade in human lung epithelial cells. Exp Mol Med **39**, 97, 2007.

48. Sun, B., Zhang, D., Zhang, S., Zhang, W., Guo, H., andZhao, X. Hypoxia influences vasculogenic mimicry channel formation and tumor invasion-related protein expression in melanoma. Cancer Lett **249**, 188, 2007.

49. Koong, A.C., Denko, N.C., Hudson, K.M., Schindler, C., Swiersz, L., Koch, C., Evans, S., Ibrahim, H., Le, Q.T., Terris, D.J., andGiaccia, A.J. Candidate genes for the hypoxic tumor phenotype. Cancer Res **60**, 883, 2000.

50. Kondo, S., Kubota, S., Shimo, T., Nishida, T., Yosimichi, G., Eguchi, T., ... & Takigawa, M. . Connective tissue growth factor increased by hypoxia may initiate angiogenesis in collaboration with matrix metalloproteinases. Carcinogenesis 2002.

51. Zhu, Z., Yin, J., Guan, J., Hu, B., Niu, X., Jin, D., Wang, Y., andZhang, C. Lithium stimulates human bone marrow derived mesenchymal stem cell proliferation through GSK-3beta-dependent beta-catenin/Wnt

pathway activation. Febs j **281**, 5371, 2014.

52. Peng, F., Wang, J.H., Fan, W.J., Meng, Y.T., Li, M.M., Li, T.T., Cui, B., Wang, H.F., Zhao, Y., An, F., Guo, T., Liu, X.F., Zhang, L., Lv, L., Lv, D.K., Xu, L.Z., Xie, J.J., Lin, W.X., Lam, E.W., Xu, J., andLiu, Q. Glycolysis gatekeeper PDK1 reprograms breast cancer stem cells under hypoxia. Oncogene **37**, 1119, 2018.

53. Jeter, C.R., Yang, T., Wang, J., Chao, H.P., andTang, D.G. Concise Review: NANOG in Cancer Stem Cells and Tumor Development: An Update and Outstanding Questions. Stem Cells **33**, 2381, 2015.

54. Cioffi, M., D'Alterio, C., Camerlingo, R., Tirino, V., Consales, C., Riccio, A., Ierano, C., Cecere, S.C., Losito, N.S., Greggi, S., Pignata, S., Pirozzi, G., andScala, S. Identification of a distinct population of CD133(+)CXCR4(+) cancer stem cells in ovarian cancer. Sci Rep **5**, 10357, 2015.

55. Aso, T., Matsuo, M., Kiyohara, H., Taguchi, K., Rikimaru, F., Shimokawa, M., Segawa, Y., Higaki, Y., Umeno, H., Nakashima, T., andMasuda, M. Induction of CD44 variant 9-expressing cancer stem cells might attenuate the efficacy of chemoradioselection and Worsens the prognosis of patients with advanced head and neck cancer. PLoS One **10**, e0116596, 2015.

56. Kreso, A., andDick, J.E. Evolution of the cancer stem cell model. Cell Stem Cell **14**, 275, 2014.

57. Zhang, P., Zhang, M., Yu, D., Liu, W., Hu, L., Zhang, B., Zhou, Q., andCao, Z. Lycorine inhibits melanoma cell migration and metastasis mainly through reducing intracellular levels of beta-catenin and matrix metallopeptidase 9. J Cell Physiol 2018.

58. Shiraishi, A., Tachi, K., Essid, N., Tsuboi, I., Nagano, M., Kato, T., Yamashita, T., Bando, H., Hara, H., andOhneda, O. Hypoxia promotes the phenotypic change of aldehyde dehydrogenase activity of breast cancer stem cells. Cancer Sci **108**, 362, 2017.

59. Ramteke, A., Ting, H., Agarwal, C., Mateen, S., Somasagara, R., Hussain, A., Graner, M., Frederick, B., Agarwal, R., andDeep, G. Exosomes secreted under hypoxia enhance invasiveness and stemness of prostate cancer cells by targeting adherens junction molecules. Mol Carcinog **54**, 554, 2015.

60. Finger, E.C., Castellini, L., Rankin, E.B., Vilalta, M., Krieg, A.J., Jiang, D., Banh, A., Zundel, W., Powell, M.B., andGiaccia, A.J. Hypoxic induction of AKAP12 variant 2 shifts PKA-mediated protein phosphorylation to enhance migration and metastasis of melanoma cells. Proc Natl Acad Sci U S A **112**, 4441, 2015.

61. Keith, B., Johnson, R.S., andSimon, M.C. HIF1alpha and HIF2alpha: sibling rivalry in hypoxic tumour growth and progression. Nat Rev Cancer **12**, 9, 2011.

62. Paschall, A.V., Yang, D., Lu, C., Redd, P.S., Choi, J.H., Heaton, C.M., Lee, J.R., Nayak-Kapoor, A., andLiu, K. CD133+CD24lo defines a 5-Fluorouracil-resistant colon cancer stem cell-like phenotype. Oncotarget **7**, 78698, 2016.

63. Douillard, J.Y., Cunningham, D., Roth, A.D., Navarro, M., James, R.D., Karasek, P., Jandik, P., Iveson, T., Carmichael, J., Alakl, M., Gruia, G., Awad, L., andRougier, P. Irinotecan combined with fluorouracil compared with fluorouracil alone as first-line treatment for metastatic colorectal cancer: a multicentre randomised trial. Lancet **355**, 1041, 2000.

64. Li, L.N., Zhang, H.D., Yuan, S.J., Tian, Z.Y., Wang, L., andSun, Z.X. Artesunate attenuates the growth of human colorectal carcinoma and inhibits hyperactive Wnt/beta-catenin pathway. Int J Cancer **121**, 1360, 2007.

65. Tong, Y., Liu, Y., Zheng, H., Zheng, L., Liu, W., Wu, J., Ou, R., Zhang, G., Li, F., Hu, M., Liu, Z., andLu, L. Artemisinin and its derivatives can significantly inhibit lung tumorigenesis and tumor metastasis through Wnt/beta-catenin signaling. Oncotarget **7**, 31413, 2016.

66. Rasheed, S.A., Efferth, T., Asangani, I.A., andAllgayer, H. First evidence that the antimalarial drug artesunate inhibits invasion and in vivo metastasis in lung cancer by targeting essential extracellular proteases.

Int J Cancer **127**, 1475, 2010.

67.   Mak, I.W., Evaniew, N., andGhert, M. Lost in translation: animal models and clinical trials in cancer treatment. Am J Transl Res **6**, 114, 2014.

68.   Jackson, S.J., andThomas, G.J. Human tissue models in cancer research: looking beyond the mouse. Dis Model Mech **10**, 939, 2017.

69.   Mittal, V.K., Bhullar, J.S., andJayant, K. Animal models of human colorectal cancer: Current status, uses and limitations. World J Gastroenterol **21**, 11854, 2015.

Supplemental figures

Fig S1. Promoter analysis of MMP9 in human and mouse. (A) Maps of MMP9 promoter regions in human and mouse. (B) Alignment of the MMP9 promoter sequences in human and mouse. Consensus binding sites for GR, NF-κB, TCF-4/LEF-1, as well as a TPA-response element, TATA box, transcription start site (+1), and first ATG were mapped.

Fig. S2. Fluorometric reporter assay. (A) Transfection efficiencies to Colon26 and LuM1. The cells were transfected with pCMV-GFP using electroporation. Mean ± SD, n=4. (B) Representative fluorescence images at 24 h post-transfection of pZsGreen/Mmp9-promo using electroporation (right) and non-electroporation negative control (NC, left). DNA was stained with NucBlue. Scale bars, 200 μm.
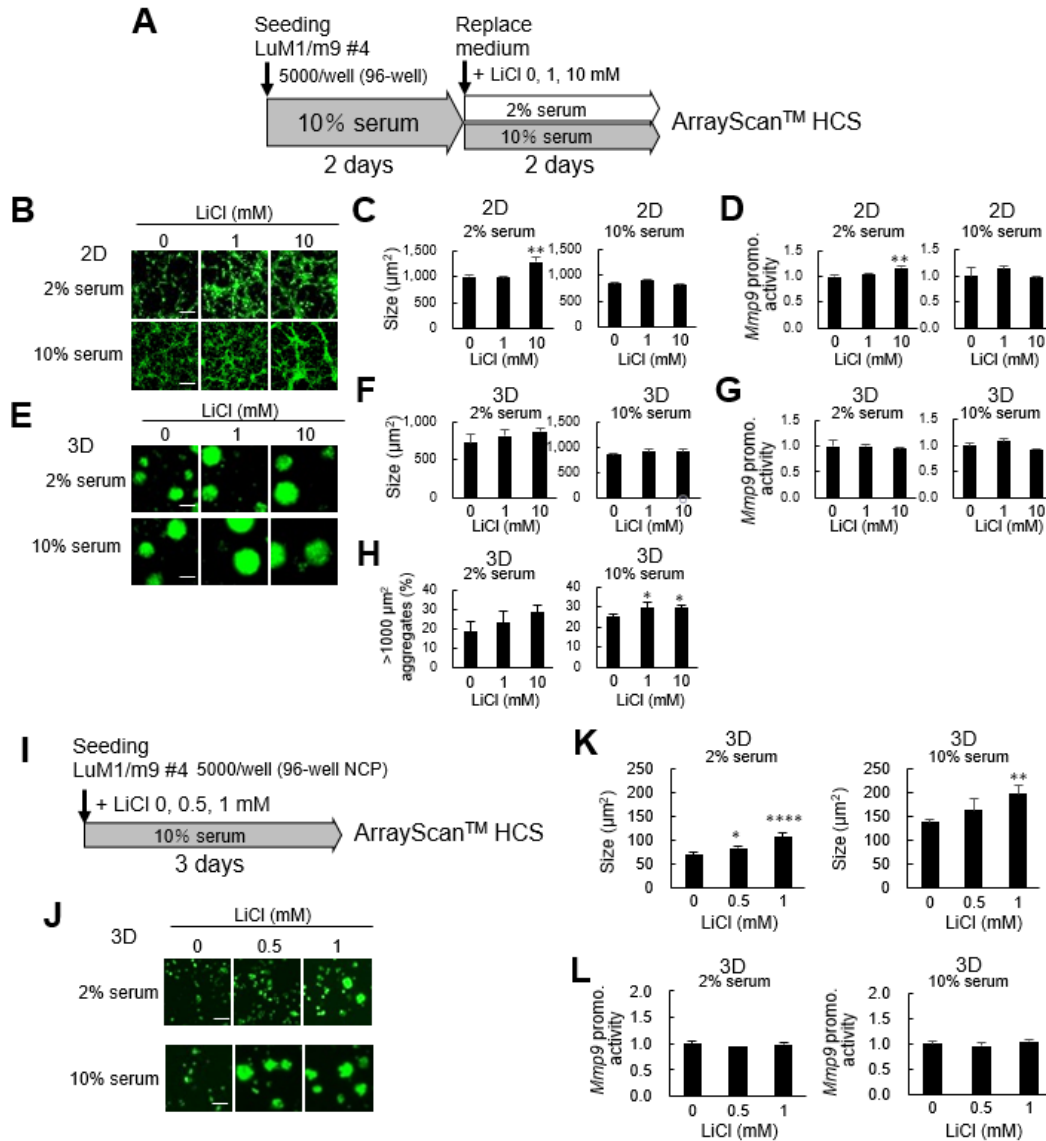
Fig. S3. Effects of LiCl on the LuM1/m9 reporter cells in various conditions. (A) Schemed protocols of LiCl treatment used for "B to H". LuM1/m9 #4 were pre-cultured in RPMI1640 medium with 10% serum before LiCl administration in 2D or 3D culture plates. (B and C) Representative fluorescent reporter images of cell-aggregates. Scale bars, 100 μm. (D and F) Size of cell-aggregates. Mean ± SD, n=3. **$P<0.01$ vs non-treated control group. (E and G) *Mmp9* promoter activities per cell-aggregates. Mean ± SD, n=3. **$P<0.01$ vs non-treated control group. (H) The rate of cell-aggregates larger than 1000 μm^2 in a 96-well plate. Mean ± SD, n=3. *$P<0.05$ vs non-treated control group. (I) Schemed protocols of LiCl treatment used for "J to L". LuM1/m9 #4 were seeded in RPMI1640 medium supplemented with 0, 0.5 or 1 mM LiCl and 2 or 10% serum in NCP. (J) Representative fluorescent reporter images of cell-aggregates. Scale bars, 100 μm. (K) Size of cell-aggregates. Mean ± SD, n=3. *$P<0.05$, **$P<0.01$, ****$P<0.0001$ vs non-treated control group. (L) *Mmp9* promoter activities per cell-aggregates. Mean ± SD, n=3. The data of "2D 2% serum" condition shown in B, C, and E, and the data of "3D 2% serum" condition shown in J, K, and L were also shown in Fig. 3.
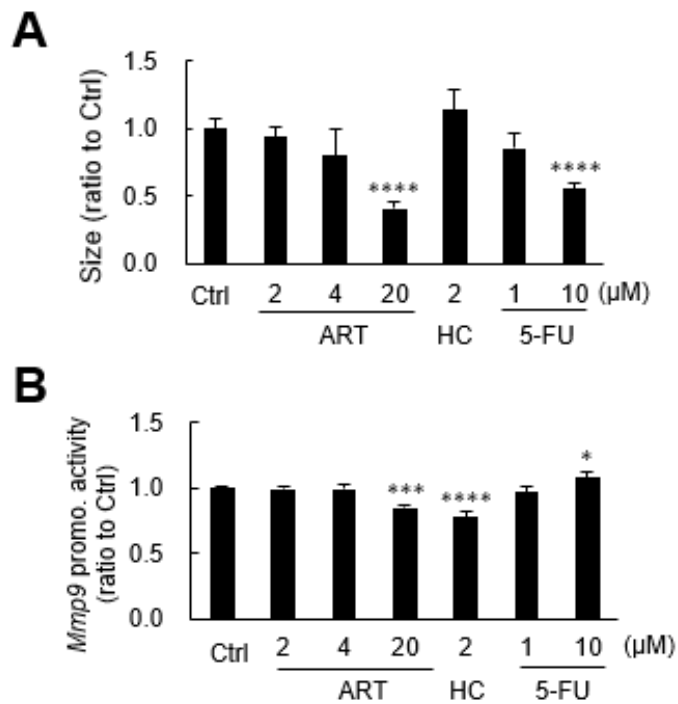
Fig. S4. Effects of ART, HC, and 5-FU on tumorigenesis and the *Mmp9* promoter activity.
To investigate the effects of HC, 5-FU, and ART, cells were seeded at a concentration of 5×10^3 cells/well in a 96-well NCP, and cultured in stem-cell medium for 3 days with or without drugs. (A) The rate of tumoroid size. Mean ± SD, n=3-4. ****P<0.0001 vs non-treated control group (Ctrl). (B) *Mmp9* promoter activities per cell-aggregates. Mean ± SD, n=3-4. *P<0.05, ***P<0.001, ****P<0.0001 vs Ctrl.
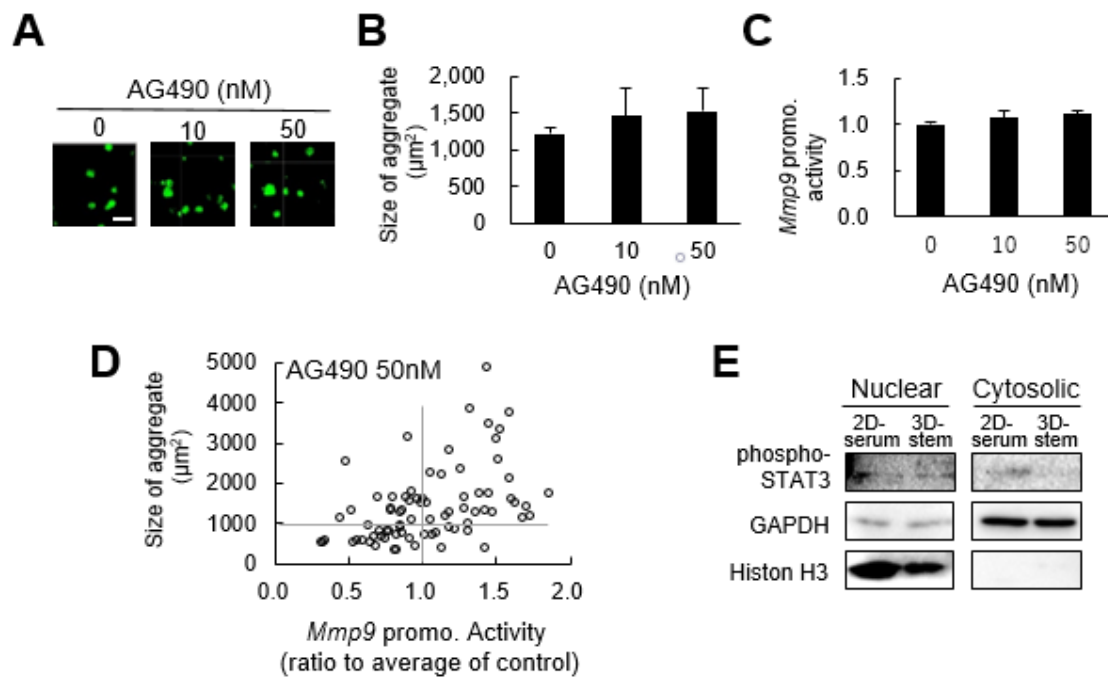
Fig. S5. STAT inhibitor (AG490) did not alter tumorigenesis and the *Mmp9* promoter activity in vitro. (A) Representative fluorescent reporter images of tumoroids. Scale bars, 100 μm. (B) Size of cell-aggregates. Mean ± SD, n=4. (C) *Mmp9* promoter activities per cell-aggregates. Mean ± SD, n=4. (D) Scatter plot analysis of all tumoroids in each well. All tumoroids were plotted according to their size (horizontal axis) and the fluorescence intensities per pixel (=μm^2) (vertical axis). (E) Western blot analysis of phospho-STAT3 in nuclear and cytoplasmic fractions. Histone H3 was blotted as a marker of nuclei. GAPDH was blotted as a marker of cytoplasm. The same images of Histone H3 and GAPDH were shown in Fig. 3E.